CONF-811040--200

CONF-811040--200

DE83 008509

Paper to be presented at the 9th Symposium on Engineering Problems of Fusion Research, Chicago, Illinois, October 26-29, 1981

CONCEPTUAL DESIGN OF THE INTOR FIRST-WALL SYSTEM*

D. L. Smith, S. Majumdar, R. F. Mattas,
L. Turner, J. Jung and M. A. Abdou

Fusion Power Program
Argonne National Laboratory
Argonne, Illinois 60439

D. Bowers and C. Trachsel
McDonnell Douglas Astronautics Company
St. Louis, Missouri 63166

B. Merrill
EG&G Idaho, Inc.,
Idaho Falls, Idaho 83401

October 1981

*Work supported by the U.S. Department of Energy.

CONCEPTUAL DESIGN OF THE INTOR FIRST-WALL SYSTEM*

D. L. Smith, S. Majumdar, R. F. Mattas, L. Turner, J. Jung and M. A. Abdou

Fusion Power Program
Argonne National Laboratory
Argonne, Illinois 60439

D. Bowers and C. Trachsel
McDonnell Douglas Astronautics Company
St. Louis, Missouri 63166
B. Merrill
EG&G Idaho, Inc.,
Idaho Falls, Idaho 83401

Abstract

The design concept and performance characteristics of the first-wall design for the phase-1 INTOR (International Tokamak Reactor) study is described. The reference design consists of a water-cooled stainless steel panel. The major uncertainty regarding the performance of the bare stainless steel wall relates to the response of a thin-melt layer predicted to form on limited regions during a plasma disruption. A more-complex backup design, which incorporates radiatively cooled graphite tiles on the inboard wall, is briefly described.

Introduction

A major effort of the INTOR (International Tokamak Reactor) study was focused on the design and performance of the first wall system. Several options were proposed and the key issues were addressed in considerable detail. The analyses performed by the four "countries" during phase 1 are documented in the reports issued by EC[1], Japan[2], USA[3] and USSR[4]. Additional information on the materials data base assessment was reported in the phase-0 report [5]. This report describes the design concept and presents the performance characteristics of the reference design, which is a bare stainless steel wall. A backup design, which is similar to the reference design but has radiatively cooled graphite tiles on the inboard wall, is briefly described.

The first-wall system as defined in the present study, which generally consists of the plasma chamber and serves as the first physical barrier for the plasma, consists of the following components:

- an outboard wall that serves as the major fraction of the plasma chamber surface and receives particle and radiation heat loads from the plasma and radiative heating from the divertor.
- an inboard wall that receives radiative and particle flux during the plasma burn and the major fraction of the plasma energy during a disruption.
- a limiter region on the outboard wall that serves to form the plasma edge during the early part of start-up.
- a beam shine-through region on the inboard wall that receives shine-through of the neutral beams at the beginning of neutral injection.
- ripple armor on the outboard wall that receives enhanced particle fluxes caused by ripple effects during the late stages of neutral injection.

Operating parameters

The reference operating schedule for INTOR based on three stages of operation is given in Table 1. Stage 1A is a one-year hydrogen plasma operation for engineering checkout. Stage 1B consists of two years of DT plasma operation. Stage II consists of four years of engineering testing and Stage III consists of 8 years of upgraded engineering testing. The fluences and wall loadings are based on 100-s shots with a 70% duty cycle in Stage 1 and on 200-s shots with an 80% duty cycle in Stages II and III. The plasma burn produces a 620-MWt flattop power profile with an average neutron wall loading of 1.3 MW/m^2. The

Table 1. Operating Scenario for INTOR

	Availability (%)	Cycles	Burn Time (s)	Fluence	Number of Disruptions	Disruption Limit
Stage 1						
Year 1	10	3.1×10^4	2.3×10^6	2.3×10^6	115	--
Years 2-3	15	9.3×10^4	6.8×10^6	6.8×10^6	460	3.4×10^{23}
Stage 2						
Per Year	25	2.5×10^4	6.3×10^5	9.4×10^5	38	9.4×10^{23}
Years 4-7	25	31.6×10^4	25.4×10^6	12.6×10^6	126	12.6×10^{24}
Stage 3						
Per Year	50	15.8×10^4	12.6×10^6	6.2×10^6	63	6.3×10^{24}
Years 8-15	50	127.0×10^4	101.0×10^6	49.6×10^6	504	5.1×10^{25}
Lifetime	--	221.0×10^4	175.0×10^6	71.9×10^6	1093	7.1×10^{25}

fluences listed represent a peaking factor of 1.2 at the outboard regions where the test modules are located. The requirement for Stage III is to accumulate 15 MW-y/m^2 within 8 years after the end of Stage II. The annual neutron wall loading for Stage III is 0.62 MW/m^2. The parameters specified for the INTOR first wall-system are summarized in Table 2.

*Work supported by the U.S. Department of Energy.

Design Description

A poloidal view of the reference design indicating the location of the first-wall system, viz., outboard wall, inboard wall, limiter region, beam shine-through region and ripple armor region, is shown in Fig. 1. All first-wall components are fabricated from Type 316 stainless steel and utilize low-pressure (< 1 MPa) water coolant. Figure 2 is a schematic diagram of the panel-type construction showing the thicker flat panel that faces the plasma and the corrugated back panel that forms the coolant

Table 2. INTOR First-Wall Operating Parameters

Table 4. INTOR First-Wall Operating Parameters

First Wall	
Total plasma chamber area, m^2	380
Average neutron wall loading, MW/m^2	1.3
Radiative power to first wall, MW	40
Charge-exchange	
Power, MW	4
Current (50% D, 50% T), s^{-1}	1.3×10^{23}
Flux, $m^{-2}s^{-1}$	3.3×10^{20}
Energy, eV	200
Cycle time (Stage I/Stage II & III), s	145/245
Burn time (Stage I/Stage II & III), s	100/200
Total disruption energy, MJ	220
Disruption time, ms	20
Operating life, y	15 y
Total average neutron fluence, n/m^2	6.8×10^{25}
Total 14-MeV neutron fluence, MW-y/m^2	6.5
Total number shots	7.1×10^5
Total number disruptions	1080
Outboard Wall	
Area, m^2	266
Surface heat flux, W/cm^2	
From plasma	11.6
From divertor	3.4
Total	15
Average nuclear heating, W/cm^3	15
Limiter (Outboard wall at R = 6 m - Upper and Lower)	
Width, m	1
Area (each), m^2	38
Total ion flux, s^{-1}	3×10^{23}
Total heat flux, MW	10
Total ion heat flux, MW	5
Heat flux density, MW/m^2	0.3
Peaking factor	1.5
Typical particle energy, eV	100
Duration, s	4
Period, s	t = 0-4
Ripple Armor (Outboard wall at R = 6 m - Upper and Lower) (Does not coincide with the limiter.)	
Area, m^2	26
Heat flux (ripple = ±0.5%), MW/m^2	0.4
Peaking factor	2
Particle energy (D), keV	120
Period, s	t = 8-10
Inboard Wall	
Area, m^2	114 m^2
Surface heat flux, W/cm^2	11.6
Average nuclear heating, W/cm^3	10
Peak disruption energy density, J/cm^2	289
Beam-Shine-Through Region (Inboard Wall)	
Total power (5% of injected), MW	4
Particle energy, keV	175
Duration, s	2
Period, s	t = 4-6
Area, m^2	4
Heat flux, MW/m^2	1

channels. The two panels are diffusion bonded together and welded supports are spaced as required. The thickness of the plasma side panel is sufficient to withstand the sputtering and vaporization erosion predicted for the full life to the reactor. The present design philosophy was to avoid incorporating any separate armors for the special high-heat flux regions, if possible, in order to keep the first-wall system design as simple as possible. As a result, the special regions, viz., limiter, beam-shine-through and ripple-armor regions, are just a part of the first wall with minor thickness modifications to allow for effects caused by the preferential heat or particle fluxes.

The reference first-wall design is a water-cooled stainless steel panel. The low temperature water coolant maintains the structure at temperatures commensurate with acceptable structural properties under irradiation. The low pressure also tends to minimize primary stress requirements. The 20% cold-worked stainless steel is selected because of superior radiation damage resistance and the higher allowable design stress. The panel-type construction is proposed because of ease of fabrication, reduced stresses resulting from the thin corrugated coolant channels, and longer predicted lifetime than that for tube-bank designs. The outboard wall is an integral part of the blanket and serves as the containment for the neutron multiplier. This tends to minimize structure and coolant volumes between the plasma and the breeder zone, which enhances the breeding performance. The manifolding and support structure are readily incorporated with the blanket.

The reference stainless steel first-wall design meets all design requirements and is predicted to last the full reactor lifetime under the reference operating conditions. The design and lifetime analyses provided for (1) sputtering, blistering and vaporization erosion allowances, (2) maximum structural temperature limits, (3) maximum stress limits for the structure, and (4) fatigue limits of the structure. Table 3 summarizes the results of the lifetime analysis for the various regions of the first wall.

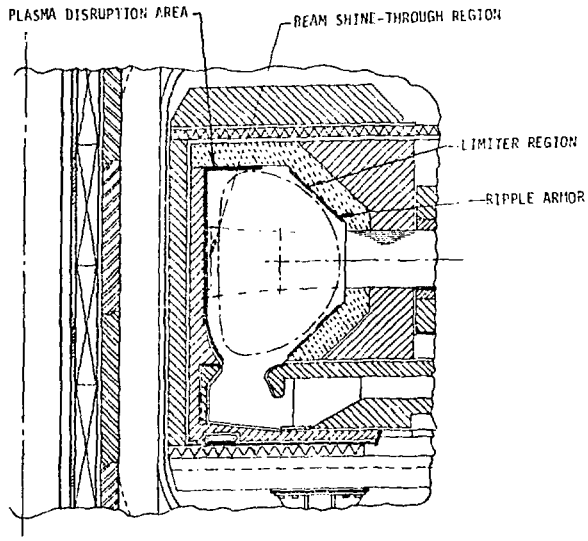

Figure 1. First-wall configuration.

The major uncertainties in the first-wall concept relate to the stability of the melt layer predicted to form during a disruption and the response of the beam shine-through region. The thin melt layer (~ 100 μm) will exist only for a short time (~10 ms).

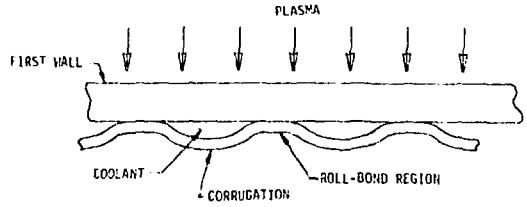

Fig. 2. First-wall cross section.

Although the calculated pressures induced in the melt layer are small, additional data are required to demonstrate that the melt region does not erode. The

lifetime analysis for the reference first-wall design does not include an allowance for erosion of the melt layer. If future investigations indicate that significant portions of the melt layer erode, design modifications of the inboard wall will be required. A possible solultion is a thick (30 mm) grooved-wall concept that would allow for erosion of f10% of the melt layer during each disruption. It should be noted, however, that the melt layer thickness and the vaporization thickness are very sensitive to the disruption conditions. Hence, any significant change in disruption conditions would most likely lead to a different design solution. A second area of major uncertainty is the beam shine-through region. A 2-s pulse exceeding 1.5 MW/m2 produces surface temperatures and fatigue damage in excess of the design limitations. Design modifications, e.g., a grooved wall, will also be required if higher heat fluxes are consistently deposited on this region.

Table 3. Summary of Lifetime Analysis

Region	Total Thickness mm	Maximum Erosion mm	Maximum[a] Temp., °C	Maximum[b] Stress MPa	Fatigue Life, cycles No Erosion	Fatigue Life, cycles W/Erosion[c]
Outboard Wall	11.7	8.7[d]	260	360	3×10^6	$>10^7$
Ripple Region	11.7	8.7[d]	297	400	1×10^6	$>10^7$
Limiter Region	12.8	9.0[d]	280	410	8×10^5	10^7
Inboard Wall	13.5	10.5[e]	275	408	9×10^5	10^7
Beam Shine-Through Region	13.5	10.5[e]	332	495	2×10^5	10^7

[a]Maximum specified temperature = 650°C.

[b]Maximum allowable stress = 660 MPa plasma side, 765 MPa coolant side (cold-worked material).

[c]Assumes erosion rate one-half of predicted rate for conservative design.

[d]Physical sputtering plus vaporization.

Materials assessment

The materials data base used for the lifetime analysis of the reference first-wall design is summarized in this section. Considerable experimental data on light-ion sputtering have been generated in recent years. Variations in sputtering yields have been attributed to surface roughness effects, impurity effects such as oxidation of beryllium, compositional differences in alloys, temperature effects, and unresolved differences between laboratories. Analytical expressions, such as those reported by Roth et al. (6) and Smith (7), have been developed to predict sputtering yields for materials and conditions where experimental data are not available. These analytical expressions generally agree with reported experimental data within a factor of 1.5. A combination of experimental data and values calculated from these analytical expressions has been used as a basis for evaluation of erosion yields for the INTOR first wall components. Table 4 summarizes the physical sputtering yields for stainless steel at 200 eV (the average particle energy on the first wall during a burn) and 100 eV (the particle energy on the limiter region during startup). The charge exchange flux on the first wall is essentially all hydrogen with insignificant contributions from helium and other impurities.

Table 5 summarizes the physical sputtering erosion rates for the various regions of the stainless steel first-wall panel. The physical sputtering erosion rates are based on effective sputtering yields of 0.017 atoms per particle at 200 eV (6.6×10^{-6} mm/s) and 0.006 atoms per particle at 100 eV (8.3×10^{-7} mm/s).

Table 4. Recommended Sputtering Yield Values for Stainless Steel

Particle Energy (eV)	Incident Particle	Yield at/ion	Fraction of Flux	Effective Yield at/ion	Fraction of Yield
200	D	0.011	50	0.0055	33
200	T	0.022	50	0.011	67
200	NET	--	--	0.017[a]	100
100	D	0.003	50	0.002	33
100	T	0.010	50	0.004	67
100	NET	--	--	0.006[b]	--

[a]corresponds to 6.63×10^{-6} mm/s.

[b]corresponds to 8.3×10^{-7} mm/s.

Table 5. Wall Thickness Requirements for the First-Wall System

	Outboard Wall and Ripple Armor Region	Inboard Wall and Beam Shine-Through Region	Limiter Region
Physical Sputtering Erosion (Burn)	8.7 mm[a]	8.7 mm	8.7 mm
Physical Sputtering Erosion (Startup)	--	--	1.1 mm[b]
Vaporization During Disruption	--	1.8 mm[c,d]	--
Remaining Wall Thickness	3.0 mm	3.0 mm	3.0 mm
Wall Thickness Required	11.7 mm	13.5 mm	12.8 mm

[a]Erosion rate = 6.6×10^{-6} mm/s (2.2×10^{-6} mm/s during Stage 1A).

[b]Erosion rate = 3.3×10^{-4} mm/shot; assumes each limiter used 50% of the time.

[c]Assumes melt layer formed during disruption does not erode.

[d]Allowance twice calculated value of 8×10^{-4} mm/disruption.

Chemical sputtering is not predicted to cause significant erosion of the stainless steel first wall under projected operating conditions. An assessment of the blistering characteristics of stainless steel under conditions in INTOR indicated that hydrogen blistering is not significant. However, a more detailed analysis is required to assess the importance of potential blistering caused by 3.5 MeV alpha particles.

Some uncertainity exists regarding the permeation of tritium through the first wall into the coolant. Compared to results from gaseous permeation studies, enhanced permeation rates may occur when energetic tritium is injected into the first wall surface.

Type 316 stainless steel in the cold-worked condition in proposed for the first wall structure. Loss of ductility caused by displacement damage and helium generation is considered to be the most important effect of irradiation on the lifetime of stainless staeel. Although annealed material meets the calculated stress requirement, the higher allowable design stress for cold-worked materials provides a significantly larger margin of safety. Cold-worked plate can readily be fabricated in the thickness required.

Under certain conditions austenitic stainless steels are susceptible to intergranular cracking when exposed to pressurized water or steam at elevated temperatures. These effects are not predicted to be excessive for the relatively low temperature (<100°C) water if the water chemistry is carefully controlled. Impurities such as dissolved oxygen, chlorides and hydroxides can lead to enhanced intergranular cracking or stress corrosion cracking. Also, sensitization of the stainless steel must be avoided. The available data base indicates that the cold-worked material is more resistant to radiation damage than the annealed material. For the predicted operating conditions, swelling, embrittlement and radiation creep are not expected to be excessive.

Disruption effects

Three effects of plasma disruptions on the first wall were analyzed in the present study, viz., vaporization of the wall, formation of a melt layer, and electromagnetic loading. A comprehensive modeling effort was undertaken and analyses performed to evaluate the extent of vaporization and melt layer formed during a plasma disruption. Figure 3 summarizes

the calculated thickness of the vaporized region and melted region of stainless steel for various energy densities. The reference condition is 289 J/cm^2 during a 20-ms disruption. The vaporized thicknesses are considered acceptable. However, if the melted layer is eroded during the disruption, the erosion rates of stainless steel would be excessive. The surface region is molten less than 30 ms and the regions 50 μm into the wall are molten for only a few milliseconds.

Preliminary analyses of the electromagnetic forces induced in the first walls and in the melted regions were conducted. Calculated pressures in the stainless steel melt zone are less than 275 N/m^2 (0.04 psi). The maximum force on an 18-mm-OD X 10-mm-ID stainless steel tube is 2.35 kN/m. The magnitude of the force reaches a maximum before melting occurs. Also, the force reverses direction and becomes compressive at ~12 ms for the reference disruption scenerio.

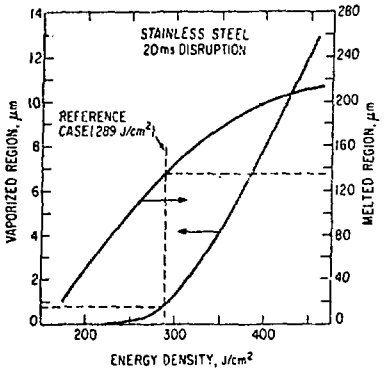

Fig. 3. Calculated vaporized and melted regions as a function of energy for a 20 ms disruption.

Thermal hydraulics

The thermal responses of the various regions of the first wall are summarized in Fig. 4 through 6 for the specified wall thicknesses and heating rates. Figure 4 shows the thermal response of the 11.7-mm outboard wall and the ripple armor region for Stage 1B operation (100-s burn). The wall temperatures remain approximately the same for the extended burn during Stage II and III operation. The maximum temperature of ~ 260°C near the end of the burn is within the 350°C maximum temperature limit specified. This temperature would be slightly less for the case of the actively cooled limiter. The 297°C thermal spike on the surface of the ripple armor region is also within the allowable temperature limits. Figure 5 shows the thermal response for the 12.8-mm thick limiter region. The temperature near the end of the burn (280°C) is slightly higher than that of the outboard wall because of the increased wall thickness; however, the 250°C thermal spike associated with startup is considerably less than the steady state temperature. The thermal response of the inboard wall is shown in Fig. 6. The higher steady-state temperature of the inboard wall (275°C) compared to the outboard wall is due primarily to the higher a bulk heating in the thicker inboard wall. The neutral beam shine-through produces a 332°C thermal spike during startup if the heat flux is 1 MW/m^2 for 2 s. A 3 MW/m^2 heat flux for the same period produces a thermal spike of ~ 700°C on the surface. Calculations indicate no thermal spike occurs at mid-thickness of the panel.

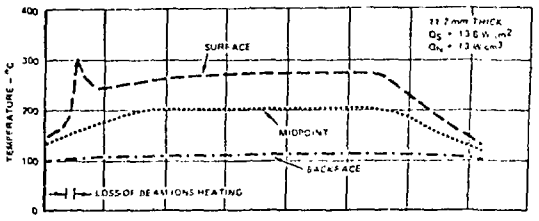

Fig. 4. Thermal Responses of Outboard Wall and Ripple Armor Region.

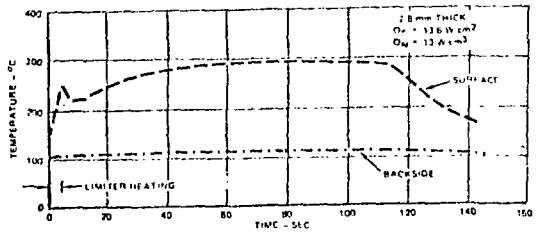

Fig. 5. Thermal Response of Limiter Region.

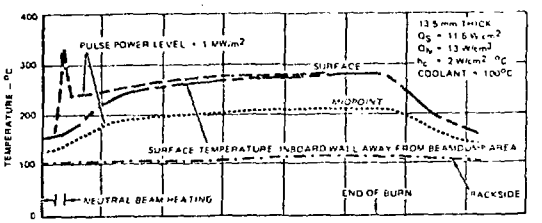

Fig. 6. Thermal Responses of Inboard Wall & Neutral Beam Shine-Through Region.

Stress/lifetime analysis

Stress and lifetime analyses have been performed to guide the design of the INTOR first wall. Pressure loading, thermal loading and magnetic loading resulting from plasma disruption have been considered in the stress analysis. The analyses have taken into account the thinning of the first wall due to sputtering and vaporization. Stresses due to differential swelling have been assumed to be small in the present analysis. Lifetime analyses under the reference operating parameters have been performed for a bare stainless steel wall as well as for stainless steel coated with beryllium. In addition to a solid first wall, the performance of a grooved first wall has also been evaluated.

For the reference operating scenario, viz., 7.1 x 10^5 cycles and 1083 disruptions over a 15-year life, a solid outboard wall constructed of an 11.7-mm-thick, 20% cold-worked stainless steel panel can meet the 15-year design life requirement for stress and fatigue life (see Table 3). The maximum allowable surface heat flux corresponding to a fatigue life of 7.1 x 10^5 cycles is shown in Fig. 7 as a function of wall thickness and the nuclear heating rate. The allowable heat flux (dotted lines) is greater than the expected heat flux in all cases. The cold-worked stainless steel provides a significantly larger design margin than annealed material for the maximum stress limit. Also, the design margin for fatigue life is substantially increased if advantage is taken of the reduced stresses that result from wall erosion. A conservative value of one-half of the predicted erosion rate gives a design life in excess of 10^7 cycles. Similar results are derived for the 12.8-mm-thick limiter region.

If the melt layer formed during a disruption does not erode, a solid inboard wall (13.5 mm) constructed of cold-worked stainless steel will meet the full 15-year design life. In order to meet the full requirement for the beam shine-through region,

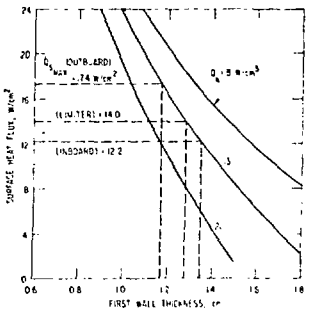

Fig. 7. Allowable maximum surface heat flux in a type 316 stainless steel wall for a fatigue life of 7.1 x 10^5 cycles, as a function of wall thickness and nuclear heating rate.

one must take advantage of the decreasing thermal stresses that result from thinning caused by erosion. If at most 10-12% of the melt layer erodes during the disruptions, a grooved stainless steel inboard wall 30 mm thick will survive the full 15-year design life.

Coolant channels can be constructed out of thin-walled (3-4 mm) corrugated panels that are welded to the back of the first wall. These panels should have sufficient fatigue life provided the water chemistry is adequately controlled to prevent early failure due to stress corrosion or corrosion fatigue.

Backup and Alternate Designs

The backup first wall concept consists of a radiatively cooled graphite liner on the 145-m^2 inboard wall with a water-cooled stainless steel panel for the outboard wall. A total of 1600 graphite tiles, each 5 cm thick by 30 cm square, are required for this design. These tiles are installed on rails and require removal of the blanket shield sector for replacement. The tiles produce 50 MW of additional nuclear heating load that must be radiated to the outboard wall and the wall behind the tiles. Tile temperatures vary from 1215°C at the start of an equilibrium burn cycle to 1320°C at the end of the cycle. The temperature of any given tile is dependent on its location and view of the cool surfaces to which it radiates.

The graphite tiles are eroded by vaporization when subjected to plasma disruptions, by chemical sputtering due to interaction with the hydrogen of the plasma, and by physical sputtering caused by high-energy plasma particle impingement. Total predicted erosion of the tiles over the life of the reactor is 30 mm. Additionally, 20 mm of graphite is required at end of life to provide adequate structure to prevent cracking due to electromagnetic loads that occur during a plasma disruption. This results in a total thickness of 50 mm. The outboard wall is made of a water-cooled Type 316 stainless steel panel that is an integral part of the blanket assembly. It is subjected to a surface heat flux of 30 W/cm^2, of which 6% W/cm^2 comes from the radiation heat load from the graphite tiles.

The major concerns regarding the graphite liner concept relate to: (1) a substantial increase in the heat flux to the outboard wall caused primarily by the nuclear heating in the graphite liner, (2) design heat flux to the outboard wall caused primarily by the complexity and difficulty associated with the mechanical support of the tiles and reliability of the tiles and supports under thermal stress and shock loading conditions; (3) stored thermal energy in the graphite liner at the high operating temperatures (1300 C); (4) chemical sputtering and redeposition of large amounts of graphite and (5) radiation damage resistance of graphite. Considerable development work is required to demonstrate the viability of the graphite liner concept.

Alternate first wall concepts considered included the use of an aluminum first-wall structure and a low-Z coating on the stainless steel first wall. A summary of the analysis for the aluminum first-wall design concept is included in the design reports [1-4]. It was concluded that, although the thermal stresses in the aluminum wall were lower than those for a stainless steel wall, stainless steel is preferable primarily because of the substantially larger melt layers formed and the much larger electromagnetic forces induced in the aluminum wall during a disruption. It is also concluded that the coated (or clad)-first-wall design concept provides flexibility in materials selection that could potentially eliminate the melt layer problem associated with the stainless steel wall and the design complexity associated with the graphite liner. Uncertainties regarding the reliability of the coating bond were identified as a major concern. If low Z coatings or claddings prove to be desirable, further research and development will be required.

References

1. "European Community Contribution to the International Tokamak Reactor Workshop," Vienna (1981).

2. "Japan Contribution to the International Tokamak Reactor Workshop," Vienna (1981).

3. "U. S. Contribution to the International Tokamak Reactor Workshop," Vienna (1981).

4. "U.S.S.R. Contribution to the International Tokamak Reactor Workshop," Vienna (1981).

5. INTOR Group, "International Tokamak Reactor - Zero Phase," International Atomic Energy Report, STI/PUB/556, Vienna (1980).

6. Roth, J., et al., "Data on Low Energy Light Ion Sputtering," Max-Planck Institut Fur Plasmaphysik, IPP 9/26 (1979).

7. Smith, D. L., J. Nucl. Mater., 75, 20 (1978); also, Proc. Workshop on Sputtering Caused by Plasma Surface Interaction, Argonne National Laboratory, p. 15-1, CONF-790775 (1979).